Available online at www.sciencedirect.com
SCIENCE DIRECT
Journal of Photochemistry and Photobiology A: Chemistry 177 (2006) 261–268
Journal of Photochemistry and Photobiology A:Chemistry
www.elsevier.com/locate/jphotochem

Preparation of TiO_2 nanocrystallites by hydrolyzing with gaseous water and their photocatalytic activity

Zhenling Wang [a,b], Liqun Mao [c], Jun Lin [a,b,*]

[a] *Key Laboratory of Rare Earth Chemistry and Physics, Changchun Institute of Applied Chemistry, Chinese Academy of Sciences, Changchun 130022, PR China*
[b] *Graduate School of the Chinese Academy of Sciences, Beijing 100049, PR China*
[c] *Laboratory of Special Functional Materials, Henan University, Kaifeng 475001, PR China*

Received 6 December 2004; received in revised form 23 April 2005; accepted 6 June 2005
Available online 27 July 2005

Abstract

TiO_2 nanocrystallites were prepared from precursors tetra-*n*-butyl titanate ($Ti(OC_4H_9)_4$) and titanium tetrachloride ($TiCl_4$). The precursors were hydrolyzed by gaseous water in autoclave, and then calcined at predetermined testing temperatures. The samples were characterized by X-ray diffraction (XRD), thermogravimetry–differential thermal analysis (TG–DTA), field emission scanning electron microscopy (FE-SEM), Fourier transform infrared spectra (FT-IR), and UV–vis diffuse reflectance spectra (DRS). The photocatalytic activities of the samples were evaluated by the photobleaching of methylene blue (MB) in aqueous solution and the photocatalytic oxidation of propylene in gas phase at ambient temperature. The results showed that the anatase phase nanocrystalline TiO_2 could be obtained at relatively low temperatures (for precursor $Ti(OC_4H_9)_4$ at 110 °C and for $TiCl_4$ at 140 °C, respectively), and that the as prepared samples exhibited high photocatalytic activities to photobleach MB in aqueous solution. As the calcination temperatures increasing, the decolor ratio of MB increased and reached the maximum value of nearly 100% at 600 °C, and then decreased. The photobleaching of MB by all samples followed the pseudo-first-order kinetics with respect to MB concentration. The photodecomposition amount of propylene by TiO_2 nanocrystallites calcined at 600 °C from precursor of $Ti(OC_4H_9)_4$ is 21.6%, which is approaching to that by Degussa P25 TiO_2 (24.9%).

Keywords: TiO_2; Gaseous water; Photocatalytic activity; Methylene blue; Propylene

1. Introduction

Since Fujishima and Honda discovered the photocatalytic splitting of water on the TiO_2 electrodes in 1972 [1], titania has been studied extensively because of its wide applications in many fields, such as solar energy conversion and storage [2], photocatalysis [3], and so on. As a photocatalyst, TiO_2 is characterized by biological and chemical inertness, strong oxidizing power, cost effectiveness, and long-term stability against photocorrosion and chemical corrosion [4], so it has been proven to be the most suitable compound for widespread environmental applications. For example, most of the contaminants in water and air can be degraded completely by photocatalysis of TiO_2 [4]. Bacteria, viruses, and cancer cells can also be destructed or inactivated via photocatalysis reaction of TiO_2 [5].

Nanocrystalline TiO_2 can be prepared in various ways. One of the most common methods is hydrolysis and condensation of titanium tetraalkoxide or titanium tetrachloride. However, the TiO_2 precursors like titanium chlorides or titanium alkoxides are quite sensitive to water, and control of the hydrolysis–condensation reactions to stabilize the colloidal particles is difficult to achieve [6]. Therefore, many researchers have taken different measures to control the relative rate of hydrolysis–condensation reactions. Barringer and Bowen [7] and Edelson and Glaeser [8] synthesized monodispersed TiO_2 powder through the

* Corresponding author. Tel.: +86 431 5262031; fax: +86 431 5698041.
E-mail address: jlin@ns.ciac.jl.cn (J. Lin).

1010-6030/$ – see front matter © 2005 Elsevier B.V. All rights reserved.
doi:10.1016/j.jphotochem.2005.06.005

controlled hydrolysis of dilute ethanolic solutions of titanium tetraethoxide. Léaustic et al. [6,9] modified titanium alkoxides ($Ti(OPr^i)_4$, $Ti(OEt)_4$) with acetylacetone for a better control of the hydrolysis–condensation reaction in sol–gel processing. Möckel et al. [10] produced anatase nanocrystals using bis (ammoium lactato) titanium dihydroxide (ALT) as start materials instead of hydrolyzing rapidly titanium alkoxides. In neutral or high pH conditions, the hydrolysis of ALT is slower and more easily controlled than titanium alkoxide decomposition. Kominami et al. [11] synthesized nanosized TiO_2 in the anatase form through hydrolysis of titanium alkoxide in toluene with water that was dissolved from the gas phase at high temperature (150–300 °C). In the hydrolysis process, H_2O did not contact with either toluene or titanium *n*-butoxide. Among precursors of preparation nanocrystalline TiO_2 powders, inorganic compounds are more economical than alkoxides. Zhang et al. [12,13] synthesized nanosized TiO_2 powder by controlling the hydrolysis of $TiCl_4$ in aqueous solution and investigated the effects of the hydrolyzing temperature and sulphate ions on the anatase–rutile transformation and crystalline morphology. Fang and Chen [14] synthesized titania powders by thermal hydrolysis of $TiCl_4$ in a mixed solvent of *n*-propanol and water, using hydroxypropyl cellulose (HPC) as a steric dispersant. Niederberger et al. [15,16] reported a nonhydrolytic procedure to synthesize nanosized titania particles. The reaction between $TiCl_4$ and benzyl alcohol results in the formation of crystalline nanoparticles with high surface areas, even at low temperatures. Addamo et al. [17] reported various methods of preparation nanostructured TiO_2 starting from $Ti(iso\text{-}OC_3H_7)_4$ or $TiCl_4$. Moreover, they investigated systematically the effects of the preparation procedures, the calcination temperatures, the different values of the specific surface areas, and the presence of HCl or HNO_3 on the photocatalytic activity of the catalysts. However, in most cases, TiO_2 powders derived from sol–gel or coprecipitation method at low temperature are amorphous. To obtain crystalline titanium dioxide, subsequent hydrothermal processing [18–20] or calcination are usually used.

In this paper, we synthesized TiO_2 nanocrstallites by hydrolyzing of $Ti(OC_4H_9)_4$ and $TiCl_4$ with gaseous water in autoclave, and the effects of calcination temperatures on TiO_2 particle size, phase composition, and their photobleaching activities of methylene blue (MB) were investigated. Methylene blue (MB) is a blue cationic thiazine dye with λ_{max} value at 664 nm. It can be detected by UV–vis spectrum with high sensitivity and the intensity of its absorption spectrum at λ_{max} value has a linear relationship with the concentration of MB in aqueous solution. So it has been used as a model reactant in semiconductor photocatalysis [21–25]. In addition, one of the possible targets for TiO_2-based photocatalysis is the elimination of indoor air pollution. Propylene is one of the major sources of indoor air pollution. So the photodecomposition of propylene in the gas phase was also used as a model reaction to evaluate the activities of the TiO_2 photocatalysts.

2. Experimental

2.1. Preparation of nanocrystalline titania powders

Titanium tetrachloride ($TiCl_4$, 99.0%, Beijing Zhonglian Chemical Industry Corporation) and tetra-*n*-butyl titanate ($Ti(OC_4H_9)_4$, 98.0%, China Medicine Shanghai Chemical Reagent Corporation) were used as starting materials without any further purification. $Ti(OC_4H_9)_4$ or $TiCl_4$, 5 ml, was added into a weighing bottle which was then set in a 50 cm^3 autoclave. In the gap between the weighing bottle and the autoclave wall, 2.0 ml of H_2O was added to. At this point, H_2O did not contact with titania precursors. The autoclaves were heated to 110 °C for $Ti(OC_4H_9)_4$ and to 140 °C for $TiCl_4$, respectively, and held at that temperature for 3 days. During the reaction, H_2O in the gap was vaporized, and hydrolyzed the precursors. After the autoclaves were cooled to room temperature, the resulting samples were dried and ground to fine powders. Part of the products was heated to a desired temperature (450–900 °C) at a rate of 5 °C min^{-1} and held at that temperature for 2 h. For comparation, the TiO_2 powders were obtained by hydrolyzing the two precursors with liquid water, and the resulting precipitations were heated along with the above-mentioned samples.

2.2. Characterization

To determine the crystal phase composition and the crystallite size of the prepared TiO_2 powders, X-ray diffraction (XRD) measurement was carried out at room temperature using Rigaku-Dmax 2500 diffractometer with Cu $K\alpha_1$ radiation ($\lambda = 0.15406$ nm). The accelerating voltage of 40 kV and emission current of 200 mA were used. The weight fractions of the anatase and rutile phases in the sample were calculated from the relative intensities of the strongest peaks corresponding to anatase and rutile phase as described by Spurr and Myers [26]:

$$\chi_A = \frac{1}{1 + 1.26(I_R/I_A)} \quad (1)$$

where χ_A is the weight fraction of anatase in the powder, while I_R and I_A are the X-ray integrated intensities of the (1 1 0) reflection of rutile and (1 0 1) reflection of anatase, respectively. The crystallite size was estimated from the Scherrer formula:

$$D = \frac{K\lambda}{\beta \cos \theta} \quad (2)$$

where D is the crystallite size, λ the wavelength of the X-ray radiation (0.1541 nm), K usually taken as 0.89, β the peak width at half-maximum height after subtraction of the equipment broadening, $2\theta = 25.3°$ and 27.4° for TiO_2 (anatase) and TiO_2 (rutile), respectively. The thermogravimetry (TG) and differential thermal analysis (DTA) were performed using a TG-DTA instrument (DT-30 Shimadzu thermal analyzer), under an air flow of 100 mL min^{-1} with a heating rate of

10 °C min^{-1} from room temperature to 1000 °C. SEM micrographs were obtained using a field emission scanning electron microscopy (FE-SEM, XL30, Philips). Infrared absorption spectra were recorded for KBr disks containing powder sample with an FT-IR Spectrophotometer (Perkin-Elmer 580B). UV–vis diffuse reflectance spectra of titania powders were obtained using a UV/vis spectrophotometer (V-550, JASCO, Japan) equipped with an integrating sphere attachment (ISV-469). $BaSO_4$ was used as a reference sample and the UV–vis diffuse reflectance spectra (DRS) were recorded in the range of 260–850 nm.

2.3. Photocatalytic activity

The photobleaching activity of MB aqueous solution by TiO_2 powders was performed at ambient temperature. Reaction suspensions were prepared by adding 0.06 g TiO_2 powders into a 100 mL of aqueous MB solution with an initial concentration of 6 mg L^{-1}. A 30 W 254 nm UV lamp was used as a light source. The average light intensity striking on the surface of suspension was about 220 μW cm^{-2}, as measured by a UV-B meter (Photoelectric Instrument Factory of Beijing Normal University) with the peak intensity of 254 nm. Prior to photobleaching, the suspension was magnetically stirred in a dark condition for 15 min to establish an adsorption/desorption equilibrium. Then, the aqueous suspension containing MB and photocatalyst were irradiated under the UV light. At the given time intervals, analytical samples were taken from the suspension and immediately centrifuged at 6000 rpm for 5 min, and then the UV–vis absorption spectra of the supernatant were measured at the V-550 UV/Vis spectrophotometer in the range of 250–750 nm.

The photodecomposition of propylene in the gas phase was conducted at room temperature using a sealed quartz glass vessel and two 4 W black-light lamps as light sources. The glass slide (10 cm × 1 cm) coated with TiO_2 photocatalysts (the mass of catalysts is of 22 mg for all samples) on the two sides was placed in the quartz glass vessel, and the UV light intensity striking on the surface of the catalysts was 0.7 mW cm^{-2} with the peak intensity of 365 nm. The mixed air containing propylene with the initial concentration of 600 ppmv (parts per million by volume) was injected into the vessel at a flow rate of 418 mL/h. The concentration of propylene was monitored by gas chromatography (Shimadzu GAS CHROMATOGRAPH GC-9A) with a flame ionization detector (FID).

3. Results and discussion

3.1. XRD

Fig. 1(a) and (b) shows the X-ray diffraction patterns of TiO_2 powders as prepared, calcined at different temperatures, and hydrolyzed by liquid water from precursors of $Ti(OC_4H_9)_4$ and $TiCl_4$, respectively. The as-synthesized

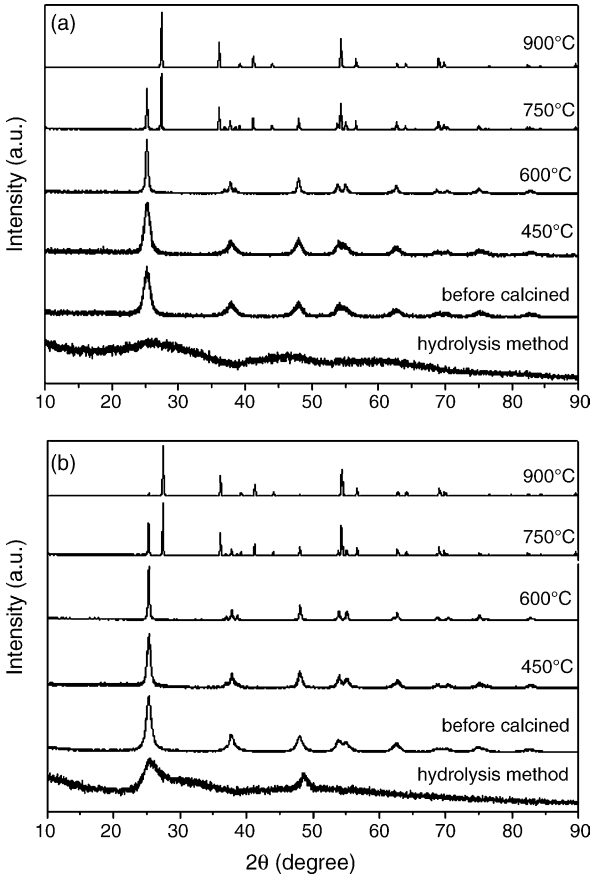

Fig. 1. X-ray diffraction patterns of TiO_2 powders as prepared, calcined at different temperatures, and hydrolyzed by liquid water from precursors of $Ti(OC_4H_9)_4$ (a) and $TiCl_4$ (b).

samples, either prepared from $Ti(OC_4H_9)_4$ or $TiCl_4$, are all in the anatase form of TiO_2. The width of the anatase (1 0 1) plane diffraction peak (2θ = 25.3°) shows wider, which indicates the formation of nanocrystallite TiO_2. Using the Scherrer equation, it is estimated that the primary particle size was 9 and 10 nm for precursors of $Ti(OC_4H_9)_4$ and $TiCl_4$, respectively. However, the structure of TiO_2 powders obtained by hydrolyzing with liquid water from the precursor of $Ti(OC_4H_9)_4$ is amorphous, and a little amount of anatase appears in TiO_2 powders from the precursor of $TiCl_4$, which may be due to the accelerating nucleation of the anatase TiO_2 by the chloride ion [19]. For samples from two precursors, with increasing calcination temperatures, the peak intensity of anatase increases and the width of the (1 0 1) peak becomes narrow, which is due to the growth of crystallites and improvement of crystallization [27]. At 600 °C, all diffraction peaks can be assigned to the anatase phase without any indication of other crystalline byproduct, which shows that the phase transition temperature of anatase to rutile is at above 600 °C. This phase transition temperature is higher than that reported by Zhang et al. [12] and lower than that reported by Kominami et al. [11]. The temperature of phase transition is affected by many factors. Under ambient conditions macrocrystalline rutile is thermodynamically stable relative

Table 1
Effects of calcination temperatures on primary particle size, phase composition, band gap energy, and rate constants of TiO_2 powders prepared from precursors $Ti(OC_4H_9)_4$ and $TiCl_4$

Calcined temperature	Particle size[a] (nm)	A[b] (%)	E_g[c] (eV)	K[d] ($\times 10^2$ min^{-1})	R[e]
$TiCl_4$					
Before-calcined	10	100	3.15	2.047	0.9981
450 °C	14	100	3.10	3.91	0.9555
600 °C	35	100	3.09	4.041	0.9981
750 °C	75 (A)	33.5	2.94	2.148	0.9974
900 °C	–	3.6	2.94	0.924	0.9906
$Ti(OC_4H_9)_4$					
Before-calcined	9	100	3.13	1.677	0.9934
450 °C	10	100	3.12	2.426	0.9892
600 °C	22 (A)	100	3.12	4.261	0.9990
750 °C	72 (A)	36.3	2.95	2.58	0.9954
900 °C	–	0	2.95	0.738	0.9855

[a] Particle size was estimated by Eq. (2), A denote the particle size of anatase form of TiO_2.
[b] The weight fractions of the anatase form (A%) in the sample were calculated by Eq. (1).
[c] Band gap energy of TiO_2 powder was obtained from the intersection of the tangent slopes according to its UV–vis spectra (Ref. [28]).
[d] Photoblenching rate constants of MB solution.
[e] Linear relative index.

to macrocrystalline anatase. However, thermodynamic stability of phase transition is particle-size dependent, and at particle diameters below ca. 14 nm, anatase is more stable than rutile [28]. In our experimental conditions, the primary particle size of TiO_2 calcined at 600 °C estimated by Scherrer equation is about 22 nm for precursor $Ti(OC_4H_9)_4$ and 35 nm for $TiCl_4$, respectively, which is larger than 14 nm and the anatase phase is still more stable than rutile. This is due to the different preparation procedure. The presence of a secondary phase, the crystallite size, the pH value of the solution, water, contaminant ions, are all the factors affecting the phase change from anatase to rutile [19,29]. When the calcination temperatures rise to 750 or 900 °C, the relative anatase phase significantly decreases due to the formation of a large amount of rutile, and the estimated primary particle size grows dramatically, which is attributable to the fact that the phase transition accelerate the process of grain growth by providing the heat of phase transformation [30]. The estimated primary particle size and composition of anatase phase are shown in Table 1.

3.2. SEM

SEM micrographs of the TiO_2 powders calcined at 450 °C prepared from precursors of $Ti(OC_4H_9)_4$ and $TiCl_4$ are shown in Fig. 2(a) and (b), respectively. The particles of two samples are spherical shapes, and the grain size of TiO_2 prepared from $Ti(OC_4H_9)_4$ is ca. 15 nm, which is smaller than that from $TiCl_4$ (25 nm). Due to the aggregate of primary particles, the particle size determined by SEM is bigger slightly than those calculated by the Scherrer equation. The reaction temperature has a great effect on the grain size of the products [18]. The higher the treatment temperature, the larger the crystallite size of the anatase TiO_2. This is one of the reasons that the crystallite size of the anatase TiO_2 treated at 110 °C for precursor of $Ti(OC_4H_9)_4$ is smaller than that of TiO_2 treated at 140 °C for precursor of $TiCl_4$. Moreover, it has been shown that the chloride ion accelerates the nucleation of the anatase TiO_2 [19], which may lead to the larger of the crystallite size of TiO_2 treated at 140 °C for precursor of $TiCl_4$. In addition, the smaller crystallite size of the TiO_2 treated at 110 °C for

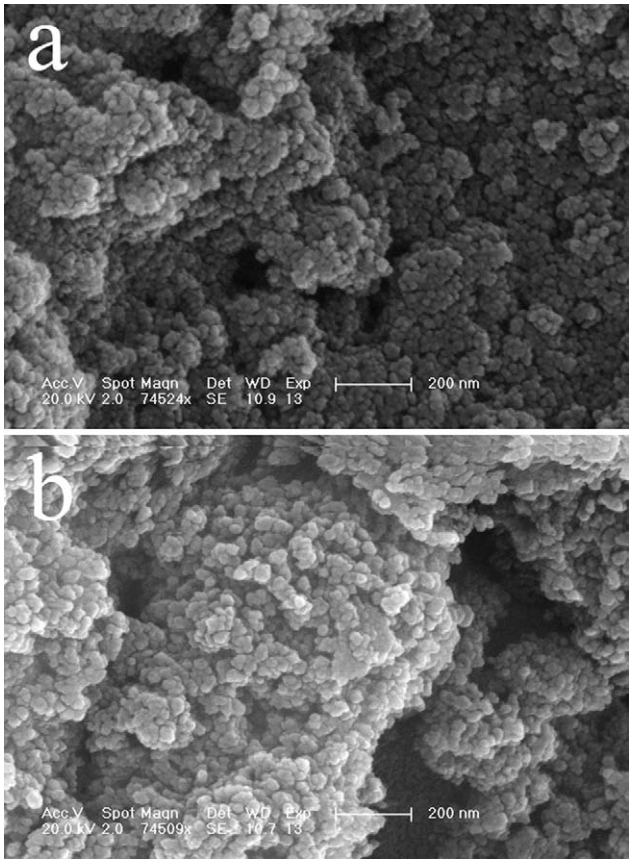

Fig. 2. FE-SEM micrographs of the TiO_2 powders calcined at 450 °C from precursors of $Ti(OC_4H_9)_4$ (a) and $TiCl_4$ (b).

precursor of $Ti(OC_4H_9)_4$ may be due to the limited solubility of TiO_2 in the organic solvent that contained a small portion of H_2O under the autoclaving conditions [11].

3.3. TG-DTA

Fig. 3 shows differential thermal analysis (DTA) and thermogravimetry (TG) curves of TiO_2 powders prepared from $Ti(OC_4H_9)_4$ (Fig. 3a) and $TiCl_4$ (Fig. 3b). In Fig. 3a, the relatively small endothermic peak is observed below 105 °C, due to desorption of the water and alcohol. A strong and broad exothermic peak at around 230 °C is attributed to the thermal decomposition of organic substances contained in the powder [30]. The TG curve is a two-step process. The first step (weight loss 2.1%) below 105 °C is due to the loss of the alcohol and the adsorbed water. The second step of weight loss (8.5%) that ranges from 105 °C to about 480 °C is attributed to the elimination of hydroxyl groups of titanium and the remains of organic substrate [15]. In Fig. 3(b), the TG curve is similar to that in Fig. 3(a), the first step of weight loss (5.2%) appeared below 118.4 °C, corresponding to the broad endothermic peak at around 55.8 °C in DTA curve, which is due to desorption of the water and remained HCl. The second step of weight loss (6.8%) that ranges from 118.4 °C to about 515.8 °C is mainly attributed to the elimination of hydroxyl groups of titanium, which is relative to the small endothermic peaks appeared at about 304 and 486 °C in the DTA curve. The exothermic peak at about 400 °C that corresponds to the crystallization of amorphous TiO_2 into anatase phase [30,31] is not appeared in both DTA curves in Fig. 3(a) and (b), which can be considered as collateral evidence to confirm the as-prepared samples to be an anatase form of TiO_2. This result is in agreement with the XRD patterns.

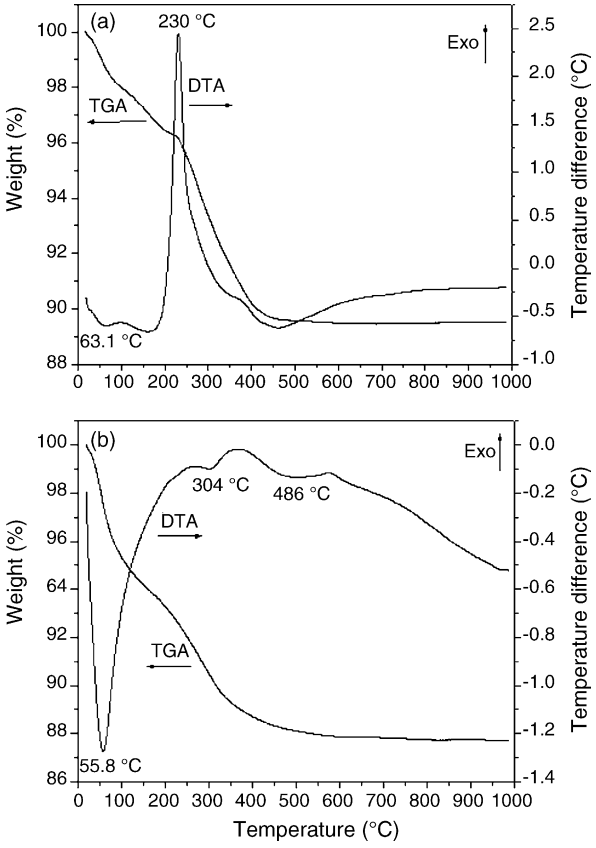

Fig. 3. TG-DTA curves of the as prepared TiO_2 powders from precursors of $Ti(OC_4H_9)_4$ (a) and $TiCl_4$ (b).

3.4. FT-IR

Fig. 4(a) and (b) shows FT-IR spectra of samples that had been prepared from different precursors and annealed at various temperatures. As the temperature was increased, the peaks in both figures corresponding to physically absorbed water (the O–H stretching mode at ~3400 cm^{-1} and the O–H bending mode at ~1640 cm^{-1}) were gradually reduced in intensity [32], while the broad peaks at 400–700 cm^{-1} corresponding to Ti–O stretching and Ti–O–Ti bridging stretching modes became narrower [27]. Even after the samples were calcined at 900 °C, very small peaks at about ~3400 and ~1640 cm^{-1} also exist, which corresponds to the hydroxyl

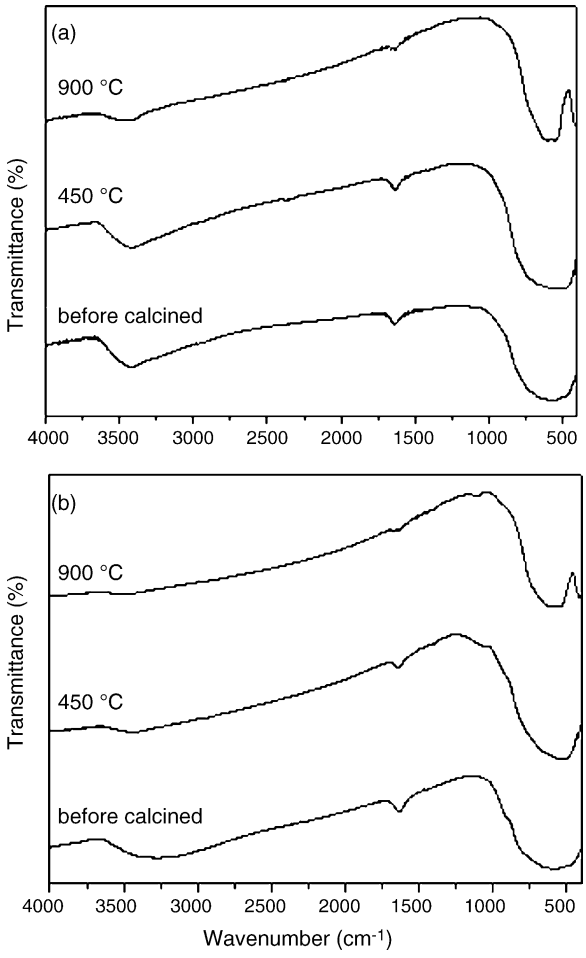

Fig. 4. FT-IR of the TiO_2 powders calcined at different temperatures from precursors of $Ti(OC_4H_9)_4$ (a) and $TiCl_4$ (b).

groups in TiO_2 powders. It can be concluded from the FT-IR results that the hydroxyl groups in TiO_2 powder can never be completely removed [27]. The shift of Ti–O stretching (from ~640 to ~465 cm^{-1}) due to the phase transition from the amorphous structure to the anatase phase of titania [32] was not observed at Fig. 4(a) and (b), which confirmed indirectly that the as prepared TiO_2 powders from the two precursors were the anatase phase of TiO_2. This is in good agreement with the results of XRD and DTA.

3.5. UV–vis diffuse reflectance spectra

Fig. 5(a) and (b) shows the diffuse reflectance spectra (DRS) of TiO_2 powders calcined at various temperatures from $Ti(OC_4H_9)_4$ and $TiCl_4$, respectively. The spectra of samples before calcination and calcined at 450 °C, 600 °C are at the similar position in both Fig. 5(a) and (b). This is attributed to the absorption of light caused by the excitation of electrons from the valence band to the conduction band of anatase phase titania [27]. With increasing the calcination temperatures, the "red shift" of DRS in Fig. 5(a) and (b) is due to the phase transformation from anatase to rutile, leading to the decrease of band gap energy. The band gap energy of samples calcined at various temperatures determined by the method Quinlan et al. [33] reported are shown in Table 1. Since the particle size of TiO_2 powders is large than ~10 nm, no "blue shift" is observed in DRS in Fig. 5(a) and (b) [34,35].

3.6. Photocatalytic activity

The photocatalytic activities of TiO_2 samples were evaluated by the photobleaching of MB in aqueous solution and the photocatalytic oxidation of propylene in gas phase. Moreover, the photocatalytic activities of TiO_2 samples were compared with commercial Degussa P25 TiO_2 and amorphous TiO_2 powders. Fig. 6 shows the changes of the decolor ratio of MB solution by samples prepared from $Ti(OC_4H_9)_4$ (a) and $TiCl_4$ (b). In both figures, without catalyst, the decolor ratio of MB due to photodecomposition after 90 min was less than 20%. TiO_2 powders obtained by hydrolyzing with liquid water from the two precursors have little photobeaching activities. However, TiO_2 nanocrystallites prepared from the two precursors have high photobeaching activities. After exposure by UV light for 90 min, the decolor ratio of MB over the two as-prepared samples is above 70%, with increasing calcination temperatures, the decolor ratio of MB increases and reaches the maximum value of nearly 100% at a calcination

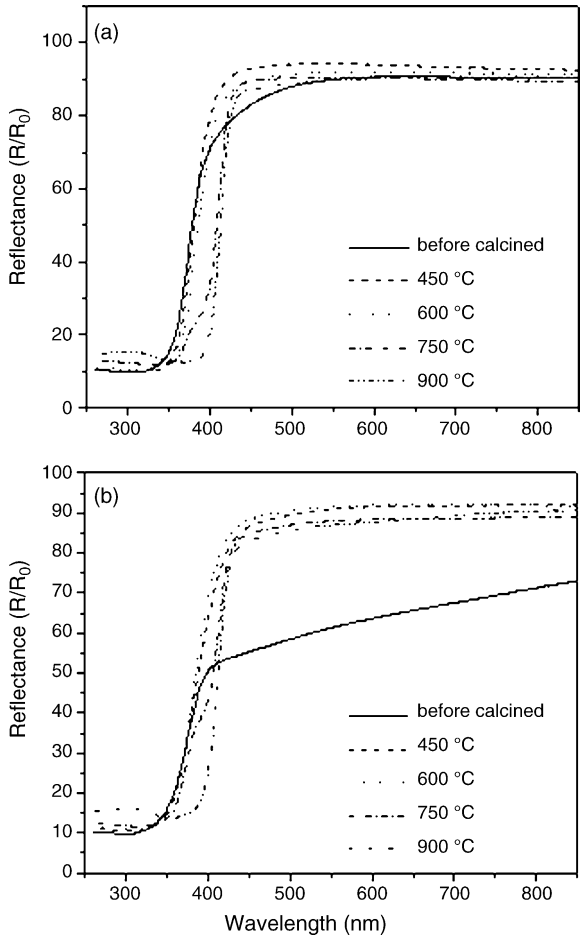

Fig. 5. UV–vis diffuse reflectance spectra of TiO_2 powders calcined at different temperatures from precursors of $Ti(OC_4H_9)_4$ (a) and $TiCl_4$ (b).

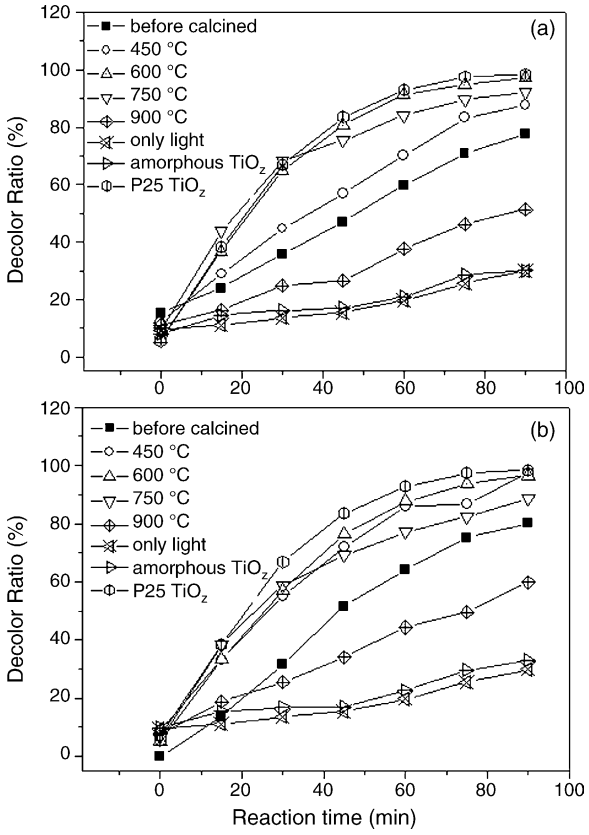

Fig. 6. Shows the changes of the decolor ratio of MB solution by samples prepared from $Ti(OC_4H_9)_4$ (a) and $TiCl_4$ (b).

Table 2
Photodecomposition amount of propylene (%) by Degussa P25 TiO_2, amorphous TiO_2, TiO_2 nanocrystallites before calcined and calcined at 600 °C prepared from precursor of $Ti(OC_4H_9)_4$

	Degussa P25 TiO_2	Amorphous TiO_2	TiO_2 before calcined	TiO_2 calcined at 600 °C
Photodecomposition amount of propylene (%)	24.9	0.0	11.3	21.6

temperature of 600 °C, and then decreases with increasing calcination temperature successively. The increase in photocatalytic activity is due to the formation of anatase and the improvement of crystallization of anatase in the samples [27], while the decrease in the photocatalytic activity of TiO_2 powders calcined at above 600 °C is due to the phase transformation of anatase to rutile and the growth of TiO_2 crystallites [27]. It also can be seen from Fig. 6, during the first 30 min of UV illumination the decoloration ratio of MB by the TiO_2 nanocrystallites increases fastly, but after that the decoloration ratio increases slowly. Under light-rich conditions, photocatalytic reaction rate depends on the adsorptive property of MB onto the catalysts surface. The more the amount of MB adsorbed onto the catalysts surface, the higher the photobleaching rate [36]. As the illumination time increasing, the amount of dye adsorbed onto the catalysts surface becomes smaller due to the photobleaching of MB by the catalysts [37]. Therefore, the decoloration ratio of MB increases slowly after the first 30 min. The photobleaching activity of MB by TiO_2 nanocrystallites calcined at 600 °C from the two precursors approaches that of commercial TiO_2 catalysts. The experimental data demonstrated that the photobleaching of MB by all samples followed the pseudo-first-order kinetics with respect to MB concentration. The observed rate constants of photobleaching of MB by various samples and the corresponding linear relative index are shown in Table 1. This is in agreement with the results reported by literatures [38,39].

Mills and Wang [22] thought that the photobleaching of MB by TiO_2-sensitised photocatalysis fall largely into two categories: (i) the reduction of MB to LMB (The doubly reduced form of MB, leuco-methylene blue (LMB), is colourless and stable in de-aerated aqueous solutions.) and (ii) the mineralisation of MB by O_2. Both reactions give the same superficial result, namely, the MB dye is bleached, the difference between the two reactions is reversible in reaction (i), (upon the addition of O_2 to the anaerobic system, which oxidizes LMB back to MB), but irreversible in reaction (ii). If the photobleaching of MB under our experimental conditions is obey to the reaction (i), as the addition of oxygen to the system, the irradiated solution should lead to some, if not total, recovery in the blue coloration due to LMB is oxidized back to MB by oxygen. However, the solution is not recovered in the blue coloration, which indicates that the reaction is obey to the second reaction (ii).

The photodecomposition amount of propylene by commercial Degussa P25 TiO_2, amorphous TiO_2 powders, TiO_2 nanocrystallites as prepared and calcined at 600 °C from the precursor of $Ti(OC_4H_9)_4$ is shown in Table 2. The amorphous TiO_2 powders have no activity for photocatalytic oxidation of propylene. The photodecomposition amount of propylene by as prepared TiO_2 nanocrystallites is about 11.3%, whereas the photodecomposition amount by TiO_2 nanocrystallites calcined at 600 °C is about 21.6%, which is approaching to that by Degussa P25 TiO_2 (24.9%). It should be denoted that the data of photocatalytic oxidation of propylene by TiO_2 nanocrystallites prepared from $TiCl_4$ precursor were not shown in Table 2 due to its abnormal behavior. This photocatalytic reaction system needs to be investigated further.

Since the literature on the synthesis of titanium oxide nanoparticles is abundant, we would like to compare our reaction system with some selected publications. It has been reported that TiO_2 nanocrystallites were obtained by a nonaqueous route even at very low synthesis temperatures [15,16], however the organic agents (such as benzyl alcohol, dopamine, and 4-*tert*-butylcatechol, etc.) used in the synthesis procedure were hazardous to environment and this method was not suited to production in large-scale. The formation of anatase nanocrystals with hot water treatment is a unique phenomenon to the silica–titania system, which was not observed in pure titania gel films with the same hot water treatment [40,41]. In the most cases for sol–gel methods, gels or precipitates obtained from the hydrolysis of titanium precursors are amorphous in nature and calcination or hydrothermal treatment is necessary to induce crystallization. The coprecipitation method also has the problem of a high crystallization temperature. The so-called chloride process industrially produces titanium dioxide. The requirements for equipment and materials are very harsh because of high reaction temperature (>1400 °C) and strong corrosiveness of Cl_2 at high temperature [18]. Though TiO_2 nanocrystallites can be obtained by hydrothermal method at relatively low temperature, the phase, morphology, and grain size of samples treated by this technique were affected by many factors, such as the temperatures, the mineralizers, the pH value, ions in solution, etc. [18,19,28]. The technique presented here can prepare a pure anatase phase without other titanium oxide polymorphs and seems an economical and simple way to obtain the TiO_2 nanocrystallites. For some reactions that hydrolyzed too seriously to be controlled, this method may be an effective means to control the hydrolysis–condensation process.

4. Conclusions

Anatase phase TiO_2 nanocrystallites were prepared by hydrolyzing titanium precursors with gaseous water in autoclave at relatively low reaction temperatures. When the as prepared samples were calcined at 450 °C, the grain size

of TiO_2 prepared from $Ti(OC_4H_9)_4$ and $TiCl_4$ is about 15 and 25 nm, respectively. At 600 °C, all diffraction peaks can be assigned to the anatase phase of TiO_2. The as prepared samples exhibited high photobleaching activities of MB in aqueous solution. With increasing calcination temperatures, the decolor ratio of MB increases and reaches the maximum value of nearly 100% at 600 °C, and then decreases. The photobleaching activity of TiO_2 nanocrystallites calcined at 600 °C from the two precursors approaches that of commercial TiO_2 catalysts. The photobleaching of MB by all samples followed the pseudo-first-order kinetics with respect to MB concentration. Moreover, TiO_2 nanocrystallites calcined at 600 °C from the precursor of $Ti(OC_4H_9)_4$ have higher photocatalytic oxidation activity of propylene in gas phase. The photodecomposition amount of propylene by this sample is about 21.6%, which is approaching to that by Degussa P25 TiO_2 (24.9%).

Acknowledgements

This project is financially supported by the foundation of "Bairen Jihua" of Chinese Academy of Sciences, the MOST of China (No. 2003CB314707), and the National Natural Science Foundation of China (50225205, 20431030). The authors thank Prof. Qinglin Li (Lanzhou Institute of Chemical and Physics, Chinese Academy of Sciences) for useful suggestions.

References

[1] K. Honda, A. Fujishima, Nature 238 (1972) 37–38.
[2] A. Hagfeldt, M. Grätzel, Chem. Rev. 95 (1995) 49–68.
[3] A.L. Linsebigler, G. Lu, J.T. Yates, Chem. Rev. 95 (1995) 735–758.
[4] M.R. Hoffmann, S.T. Martin, W. Choi, D.W. Bahnemann, Chem. Rev. 95 (1995) 69–96.
[5] A. Fujishima, T.N. Rao, D.A. Tryk, J. Photochem. Photobiol. C: Photochem. Rev. 1 (I) (2000) 1–21.
[6] A. Léaustic, F. Babonneau, J. Livage, Chem. Mater. 1 (1989) 248–252.
[7] E.A. Barringer, H.K. Bowen, Langmuir 1 (1985) 414–420.
[8] L.H. Edelson, A.M. Glaeser, J. Am. Ceram. Soc. 71 (1988) 225–235.
[9] A. Léaustic, F. Babonneau, J. Livage, Chem. Mater. 1 (1989) 240–247.
[10] H. Möckel, M. Giersig, F. Willig, J. Mater. Chem. 9 (1999) 3051–3056.
[11] H. Kominami, M. Kohno, Y. Takada, M. Inoue, T. Inui, Y. Kera, Ind. Eng. Chem. Res. 38 (1999) 3925–3931.
[12] Q.H. Zhang, L. Gao, J.K. Guo, NanoStruct. Mater. 11 (1999) 1293–1299.
[13] Q.H. Zhang, L. Gao, J.K. Guo, J. Eur. Ceram. Soc. 20 (2000) 2153–2158.
[14] C.S. Fang, Y.W. Chen, Mater. Chem. Phys. 78 (2003) 739–745.
[15] M. Niederberger, M.H. Bartl, G.D. Stucky, Chem. Mater. 14 (2002) 4364–4370.
[16] M. Niederberger, G. Garnweitner, F. Krumeich, R. Nesper, H. Cölfen, M. Antonietti, Chem. Mater. 16 (2004) 1202–1208.
[17] M. Addamo, V. Augugliaro, A.D. Paola, E. García-López, V. Loddo, G. Marcì, R. Molinari, L. Palmisano, M. Schiavello, J. Phys. Chem. B 108 (2004) 3303–3310.
[18] H. Cheng, J. Ma, Z. Zhao, L. Qi, Chem. Mater. 7 (1995) 663–671.
[19] K. Yanagisawa, J. Ovenstone, J. Phys. Chem. B 103 (1999) 7781–7787.
[20] L. Kavan, M. Kalbáč, M. Zukalová, I. Exnar, V. Lorenzen, R. Nesper, M. Graetzel, Chem. Mater. 16 (2004) 477–485.
[21] I. Bouzaida, C. Ferronato, J.M. Chovelon, M.E. Rammah, J.M. Herrmann, J. Photochem. Photobiol. A: Chem. 168 (2004) 23–30.
[22] A. Mills, J. Wang, J. Photochem. Photobiol. A: Chem. 127 (1999) 123–134.
[23] A. Houas, H. Lachheb, M. Ksibi, E. Elaloui, C. Guillard, J.-M. Herrmann, Appl. Catal. B: Environ. 31 (2001) 145–157.
[24] R. Yuan, R. Guan, W. Shen, J. Zheng, J. Colloid Interface Sci. 282 (2005) 87–91.
[25] H. Lachheb, E. Puzenat, A. Houas, M. Ksibi, E. Elaloui, C. Guillard, J.-M. Herrmann, Appl. Catal. B: Environ. 39 (2002) 75–90.
[26] R.A. Spurr, H. Myers, Anal. Chem. 29 (1957) 760–762.
[27] J.G. Yu, H.G. Yu, B. Cheng, X.J. Zhao, J.C. Yu, W.K. Ho, J. Phys. Chem. B 107 (2003) 13871–13879.
[28] H. Zhang, J.F. Banfield, J. Mater. Chem. 8 (1998) 2073–2076.
[29] J. Ovenstone, K. Yanagisawa, Chem. Mater. 11 (1999) 2770–2774.
[30] J.C. Yu, J. Yu, W. Ho, Z. Jiang, L. Zhang, Chem. Mater. 14 (2002) 3808–3816.
[31] M. Ocaňa, W.P. Hsu, E. Matijević, Langmuir 7 (1991) 2911–2916.
[32] X. Jiang, T. Herricks, Y. Xia, Adv. Mater. 15 (2003) 1205–1209.
[33] F.T. Quinlan, J. Kuther, W. Tremel, W. Knoll, S. Risbud, P. Stroeve, Langmuir 16 (2000) 4049.
[34] Y. Liu, R.O. Claus, J. Am. Chem. Soc. 119 (1997) 5273–5274.
[35] N. Serpone, D. Lawless, R. Khairutdinov, J. Phys. Chem. 99 (1995) 16646–16654.
[36] M. Miyauchi, A. Ikezawa, H. Tobimatsu, H. Irie, K. Hashimoto, Phys. Chem. Chem. Phys. 6 (2004) 865–870.
[37] M. Miyauchi, A. Nakajima, T. Watanabe, K. Hashimoto, Chem. Mater. 14 (2002) 4714–4720.
[38] X.Z. Li, F.B. Li, C.L. Yang, W.K. Ge, J. Photochem. Photobiol. A: Chem. 141 (2001) 209–217.
[39] F.B. Li, G.B. Gu, X.J. Li, H.F. Wan, Chin. J. Inorg. Chem. 17 (2001) 37–42.
[40] Y. Kotani, T. Matoda, A. Matsuda, T. Kogure, M. Tatsumisago, T. Minami, J. Mater. Chem. 11 (2001) 2045–2048.
[41] Y. Kotani, A. Matsuda, T. Matoda, T. Kogure, M. Tatsumisago, T. Minami, Chem. Mater. 13 (2001) 2144–2149.